10th World Congress on Structural and Multidisciplinary Optimization
May 19 -24, 2013, Orlando, Florida, USA

Stress-based Topology Optimization of Thermal Structures

Joshua D. Deaton[1], Ramana V. Grandhi[1]

[1] Wright State University, Dayton, Ohio, USA, deaton.13@wright.edu

1. Abstract
The majority of work in the field of topology optimization is focused on cases of maximum stiffness design for structures subjected to externally applied mechanical loads. However, this problem formulation is not suitable for a large class of problems that involve design-dependent loads, such as temperature loads, and those where stresses are of paramount concern. In fact, in addition to presenting numerical difficulties, the conventional formulation often contradicts basic design insight for thermoelastic design. The cases of thermal loading and stress constraints, even when taken individually, present additional challenges in the application of topology optimization. In this paper, we present a method for the topology optimization of structures with combined mechanical and thermoelastic (temperature) loads that are subject to stress constraints. We present the necessary steps needed to address both the design-dependent thermal loads and accommodate the challenges of stress-based design criteria. A modern stress relaxation technique is utilized to remove the singularity phenomenon in stresses and the large number of constraints that result in the optimization problem are handled using aggregation functions. We compare the results obtained using the proposed minimum volume, stress-constrained formulation versus the more conventional minimum compliance, mass constrained problems for thermoelastic structures.

2. Keywords: Thermoelastic, Topology Optimization, Stress-based Topology, Design-dependent Loading

3. Introduction
The majority of work in structural topology optimization has focused on the minimum compliance design of structures subjected to externally-applied, design-independent mechanical loading. This is likely a result of the simplicity of the structural optimization problem that arises, which due to underlying mathematics benefits from unconditionally negative sensitivities of the objective function that can be obtained at negligible computational cost [1]. From an algorithmic standpoint, this makes the numerical problem trivial to solve with modern optimizers and has enabled the solution of industrial scale topology optimization problems of hundreds or thousands of design variables and has made topology optimization a useful tool in the conceptual design of structures. However, there exists entire classes of problems that are not well addressed by this particular formulation [2].

One of these instances is the topological design of structures subject to thermoelastic effects, which are a type of design-dependent load in topology optimization. The earliest research in the area of topology optimization with thermal loads was by Rodrigues and Fernandes, who used a homogenization method to minimize the compliance of structures with combined temperature and mechanical loading [3]. The problems investigated in their work have been frequently utilized as benchmark problems in many later publications. Li et al. utilized an evolutionary method for thermoelastic topology optimization for displacement minimization [4] and problems with non-uniform temperature fields [5]. Kim et al. and Penmetsa et al. used evolutionary structural optimization (ESO) for topology design of spacecraft thermal protection system (TPS) components [6,7]. Sigmund and Torquato used topology optimization to generate structures with extremal thermal expansion properties [8] and Sigmund developed thermal micro-actuators with topology optimization [9]. In addition, Jog demonstrated topology for nonlinear thermoelasticity [10]. Since these earlier works, thermoelastic topology optimization has been performed using density-based methods to investigate the best interpolation scheme for thermal loading [11], the level set method [12], and concurrent formulations to optimize both macro and micro-scale topology [13]. Recently, Pedersen and Pedersen questioned the application of the minimum compliance problem to thermoelasticity, which is used in a number of the early research works, because it cannot achieve good performance in minimizing deformation or strength for general problems in thermoelasticity. They proposed an alternative interpolation scheme in addition to a more suitable objective function based on uniform energy density, which was shown to produce superior results from a strength design point-of-view [14,15]. The conclusion that compliance minimization is not suitable for thermoelastic problems is also supported in the work by Deaton and Grandhi, who demonstrate the inability of compliance minimization to find suitable solutions when thermal effects are significant in comparison to mechanical loads. They circumvent this problem with alternative formulations based on fictitious mechanical loads to obtain desirable thermoelastic performance for these problems [16]. In another practical application, Wang et al. proposed a multi-objective optimization model to combine low thermal directional expansion with high structural stiffness [17]. The recent abundance of alternative formulations for

thermoelastic topology optimization indicates that an increasing number of problems are not well addressed by purely compliance-based design. This is further driven by research that shows simple stiffening techniques cannot solve important problems that result from damaging thermal stresses [18]. Thus, we look to a stress-based topology design formulation to investigate its effectiveness for thermoelasticity.

Despite the fact that stresses are a primary consideration in any design problem, the topic has received little consideration in the literature compared to stiffness-based objectives until recently. This is due in large part to three primary challenges that make stress-based topological design more difficult than stiffness design. These are: (i) the singularity phenomenon, (ii) the local nature of stresses, and (iii) the highly nonlinear behavior of stress constraints [19]. Early work in the area was completed by Duysinx and Bensdoe [20,21]. More recently, Pereira et al. [22], Bruggi et al. [23,24], Guilherme and Fonseca [25], Le et al. [19], París et al [26,27], Lee et al. [28], Suresh and Takallozadeh [29], Holmberg et al. [30], and others have explored various aspects of stress-based and stress-constrained topology optimization. The particularities of the stress-constrained problem and the methods employed in this work are discussed in subsequent sections.

For the remainder of this paper, we investigate the application of a stress-constrained design formulation to thermoelastic structures. We draw relevant comparisons in both performance and results to minimum compliance for thermoelasticity. In Section 4 we present the thermoelastic finite element analysis and its parameterization for topology optimization using interpolations and filtering. Section 5 gives the mathematical formulations for both minimum compliance and stress-constrained topology optimization problems and the methods used to accommodate stress constraints. Demonstration of the methods are given in Section 6 and summary remarks and conclusions are provided in Section 7.

4. Thermoelastic FEA and Parameterization

In this section, we present the finite element analysis, material interpolation, and filtering utilized to analyze and parameterize the structural domain including considerations for the design-dependent thermoelastic loading.

4.1. Finite Element Analysis

A generalized thermoelastic structural domain Ω is given in 2D in Figure 1 that contains fixed displacement boundary conditions, externally applied surface traction forces, and a temperature change that may be uniform or spatially varying. The domain consists of regions of fixed void material, fixed solid material (non-designable), and designable areas whose topology is determined from optimization.

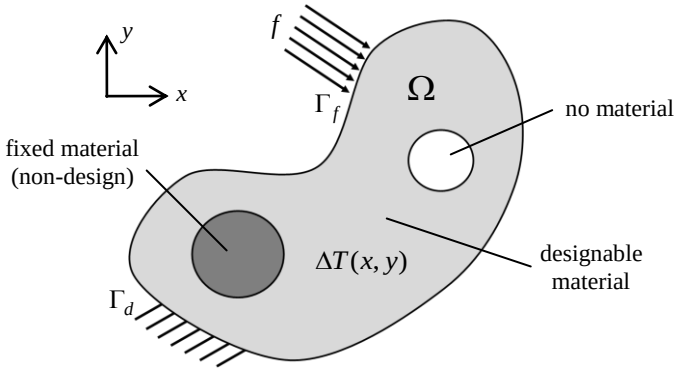

Figure 1: Generalized structural domain Ω with boundary conditions, external loading, and applied temperature.

The design domain is discretized by N finite elements, with each element assigned a design variable x_e ranging from $0 < x_e \leq 1$ with $e = 1,2,\ldots,N$. These design variables represent the relative density of the elements and form the design variable vector $\mathbf{x}$. Linear static equilibrium in a finite element system including both mechanical and thermal loading is then given by

$$\mathbf{K}(\mathbf{x})\mathbf{U} = \mathbf{F}^m + \mathbf{F}^{th}(\mathbf{x}). \tag{1}$$

Here $\mathbf{K}(\mathbf{x})$ is the stiffness matrix, $\mathbf{U}$ is the displacement vector, $\mathbf{F}^m$ is the externally applied mechanical loading, and $\mathbf{F}^{th}(\mathbf{x})$ is the thermal load vector. $\mathbf{K}(\mathbf{x})$ is assembled in the usual way as the sum over finite element stiffness matrices. The element stiffness matrices are identically to the work of Sigmund using methods consistent with typical density-based topology optimization [1]; however, the RAMP interpolation scheme is utilized as

discussed in the following section. The design-dependent thermal load vector $\mathbf{F}^{th}(\mathbf{x})$, is parameterized using the thermal stress coefficient (TSC) to maintain compatibility between stiffness and thermal force terms [11]. The nodal load vector due to temperature effects for the element e may be written as

$$\mathbf{f}_e^{th} = \int_{\Omega_e} \mathbf{B}_e^T \mathbf{C}_e \boldsymbol{\varepsilon}_e^{th} d\Omega_e \,. \tag{1}$$

By definition, $\mathbf{B}_e$ is the element strain-displacement matrix, which consists of derivatives of the element shape functions that are independent of topology design variables. $\mathbf{C}_e$ is the element elasticity matrix, which for isotropic materials can be written as a linear function of elastic modulus

$$\mathbf{C}_e = E(x_e)\overline{\mathbf{C}}_e \tag{2}$$

where $\overline{\mathbf{C}}_e$ consists of constant terms related to the material constitutive relationship, which is taken as isotropic in this work, and $E(x_e)$ is determined via a material interpolation scheme using the elemental design variable x_e. Interpolation is discussed in Section 5. $\boldsymbol{\varepsilon}_e^{th}$ is the thermal strain vector for the element given by

$$\boldsymbol{\varepsilon}_e^{th} = \alpha(x_e)\Delta T_e \boldsymbol{\phi}^T \,. \tag{3}$$

Here, $\alpha(x_e)$ is the thermal expansion coefficient of the material, ΔT_e is the temperature change on the element, and ϕ is $[1,1,1,0,0,0]$ for three-dimensions and $[1,1,0]$ for two-dimensions. Substitution of Eqs. (2) and (3) into Eq. (1) yields

$$\mathbf{f}_e^{th} = E(x_e)\alpha(x_e)\Delta T_e \int_{\Omega_e} \mathbf{B}_e^T \overline{\mathbf{C}}_e \boldsymbol{\phi}^T d\Omega_e \,. \tag{4}$$

We note that both $\alpha(x_e)$ and $E(x_e)$ are dependent upon the topological design variables and thus both necessitate material interpolation. If taken individually, the design dependence of the load vector becomes quadratic, which may introduce incompatibilities with the linear design dependence of the stiffness matrix. This is avoided by introducing the thermal stress coefficient (TSC), which is the product of the elastic modulus and coefficient of thermal expansion as

$$\beta(x_e) = E(x_e)\alpha(x_e) \,. \tag{5}$$

The TSC is then treated as an inherent material property and a single interpolation is applied to parameterize the thermal loading. Thus, $\mathbf{f}_e^{th}$ can be rewritten as

$$\mathbf{f}_e^{th} = \beta(x_e)\Delta T_e \int_{\Omega_e} \mathbf{B}_e^T \overline{\mathbf{C}}_e \boldsymbol{\phi}^T d\Omega_e \,. \tag{6}$$

where $\beta(x_e)$ varies with x_e to accommodate the design dependency of thermal loading and the remainder of the relationship is constant with respect to design variables in the optimization.

After first solving Eq. (1) to determine the displacements, the element stress tensor is determined as a post processing step from

$$\boldsymbol{\sigma}_e = \mathbf{C}_e \mathbf{B}_e \mathbf{U}_e - \mathbf{C}_e \boldsymbol{\varepsilon}_e^{th} \,. \tag{7}$$

In addition, to allow for comparison to conventional stiffness-based design objectives, the compliance C in the thermoelastic system is computed as

$$C = (\mathbf{F}^m + \mathbf{F}^{th}(\mathbf{x}))^T \mathbf{U} = \mathbf{U}^T \mathbf{K}(\mathbf{x}) \mathbf{U} \,. \tag{8}$$

4.2. Material Interpolation

The selection of the material interpolation scheme for topology optimization in the presence of design-dependent loading is extremely important. While the most popular interpolation scheme is undoubtedly the Solid Isotropic Material with Penalization (SIMP) method, it has been shown to introduce undesirable parasitic effects in optimal solutions for these types of problems. This primarily occurs because the SIMP model becomes insensitive at densities near zero and the volume constraint may not be active at the optimum design when using compliance or stiffness based objectives for design-dependent loads. An alternative interpolation introduced by Stolpe and Svanberg, called the Rational Approximation of Material Properties (RAMP) [31], which does not have zero

sensitivity at zero density, has demonstrated superior performance for problems with design-dependent loads [32,11]. In addition, a more general interpolation model, the NLPI model, that is useful with thermoelastic effects was proposed by Pedersen and Pedersen [15]. The basic form of the penalization function for the RAMP model is given as

$$R(x_e) = \frac{x_e}{1+q(1-x_e)} \tag{9}$$

where q is the penalization parameter. The parameterization for elastic modulus E and thermal stress coefficient β are given by Eqs. (10) and (11) where subscript zero denotes the value of the physical quantity for solid material and each has its own penalization parameter q_E and q_β, respectively.

$$E(x_e) = \frac{x_e}{1+q_E(1-x_e)} E_0 \tag{10}$$

$$\beta(x_e) = \frac{x_e}{1+q_\beta(1-x_e)} \beta_0 \tag{11}$$

4.3. Density Filtering

In order to prevent checker-boarding, mesh dependence, and enforce length scale in topology optimization, we employ the basic density filter of Bruns and Tortorelli [33]. This is done primarily because, in comparison to the sensitivity filter [1], the sensitivities of objectives and constraints remain numerically consistent with the optimization problem statement. This is important because more accurate sensitivity information improves optimization convergence, especially with the significant nonlinearity of stresses in topology optimization, which are used as constraints in this work. A compact form of the density filter is given by

$$\hat{x}_e = \frac{1}{\sum_{i\in N_e} H_{ei}} \sum_{i\in N_e} H_{ei} x_i \tag{12}$$

where $\hat{x}_e$ is now referred to as the physical density, N_e is the set of elements i for which the center-to-center distance $\Delta(e,i)$ to element e is smaller than the filter radius $r_{\min}$ and H_{ei} is a weight factor given by

$$H_{ei} = \max(0, r_{\min} - \Delta(e,i)) \tag{13}$$

It is also important to note that after application of the density filter, the physical density and design variable density are no longer equivalent. Thus, optimum density results given are taken as the physical density, which is consistent practice when employing a density filter or a projection scheme.

5. Topology Optimization Formulations

In the following sections, both the minimum compliance, volume constrained and minimum volume, stress constrained topology optimization problem formulations are presented. The techniques utilized to handle stress constraints in topology optimization are discussed as well.

5.1. Minimum Compliance, Volume Constrained Problem

The typical formulation for topology optimization is to identify the maximum stiffness structure by minimizing the total or mean compliance subject to a constraint on maximum allowable material. The optimization problem corresponding to the minimization of total compliance is stated as

$$\begin{aligned} \text{min:} \quad & C = \mathbf{U}^T \mathbf{K}(\mathbf{x}) \mathbf{U} . \\ \text{subject to:} \quad & \frac{V(\mathbf{x})}{V_0} - V_f \le 0 \\ & 0 \le x_{\min} < x_e \le 1 \end{aligned} \tag{14}$$

where $V(\mathbf{x})$ is the volume of the structure using the physical density, V_0 is the total volume of the designable domain, V_f is the allowable volume fraction, and $x_{\min}$ is a small value used to prevent singularity in the finite element stiffness matrices.

5.2. Minimum Volume, Stress Constrained Problem

The basic statement for the minimum volume, stress-constrained topology optimization problem is given as

$$\begin{aligned} \text{min:} \quad & V(\mathbf{x}) = \sum_{e=1}^{N} x_e v_e \,. \\ \text{subject to:} \quad & \frac{F(\boldsymbol{\sigma}_e)}{\sigma_{\text{lim}}} - 1 \le 0 \\ & 0 \le x_{\text{min}} < x_e \le 1 \end{aligned} \tag{15}$$

where v_e is the volume of the element e, σ_{lim} is the limit stress, and $F(\boldsymbol{\sigma}_e)$ is the failure criterion for stress that is a function of the stress tensor $\boldsymbol{\sigma}_e$. In this problem formulation, failure occurs when $F(\boldsymbol{\sigma}_e) > \sigma_{\text{lim}}$. For isotropic materials, the von Mises failure criterion is the most widely used failure function and is given in two dimensions as

$$\sigma_{vm} = \sqrt{\sigma_x^2 - \sigma_x \sigma_y + \sigma_y^2 + 3\sigma_{xy}^2} \tag{16}$$

using the parts of the two dimensional element stress tensor

$$\sigma_e = \begin{Bmatrix} \sigma_x & \sigma_y & \sigma_{xy} \end{Bmatrix}^T . \tag{17}$$

In practice a modified objective function is commonly employed to further penalize intermediate density material in the design domain. The modified objective, which is utilized in this work, is given by

$$V(\mathbf{x}) = \sum_{e=1}^{N} \left(x_e v_e + 0.9 x_e (1 - x_e) \right). \tag{18}$$

The additional penalization of intermediate density material to the volume objective disappears when the physical density is equal to zero or one, which helps to improve convergence to a solid/void solution in the optimization process.

5.3. Stress Constraint Relaxation

It is recognized in topology optimization that the stress-constrained problem suffers from the so-called singularity phenomenon. The singularity phenomenon is caused because the stress computed using Eq. (7) defined previously increases without bound as the density of an element approaches zero. This behavior is analogous to the singularity phenomenon experienced in truss optimization, where the axial stress in a truss element increases without bound as the area of the truss is reduced to zero. This becomes an issue in optimization when the optimum design exists with one or several design variables equal to zero because this region of the design space cannot be reached due to large constraint violations.

Recalling that zero density corresponds to a void region, rather than infinite stress at zero element density, there should exist no stress as there is no material. Several attempts at remedying this issue have been explored based on ε-relaxation [22,23,25]. More recently, Le et al. provided a much more general approach to achieving this behavior in the stress field using a consistent stress interpolation scheme [19]. In their work, the elemental stress constraint is first rewritten as $\eta_\sigma(x_e)\sigma_{vm} \le \sigma_{\text{lim}}$ where $\eta_\sigma(x_e)$ is a continuous interpolation function and $\eta_\sigma(0) = 0$ and $\eta_\sigma(1) = 1$. The choice of interpolation function behavior must satisfy several criteria identified in the referenced paper to provide good performance. In this work, the interpolation function on stress is taken as

$$\eta_\sigma(x_e) = x_e^{1/2}, \tag{19}$$

which was shown previously to give adequate performance for purely mechanical stresses. The stress failure function in the optimization problem in Eq. 15 now becomes

$$F(\boldsymbol{\sigma}_e) = x_e^{1/2} \sigma_{vm} \tag{20}$$

when using the von Mises failure criteria. The effectiveness of this method at removing the singularity phenomenon in the topological design space is shown in Figure 2. Here, two arbitrary density distributions are given in Figure 2a and Figure 2b where white/black regions correspond to void/solid and gray regions represent any intermediate density material. The structure shown is fixed in all directions along the vertical edges of the

domain and a mechanical load is applied at the center of the bottom. A uniform elevated temperature is also applied to the entire domain. Figures 2b and 2e show the von Mises stress computed directly from the finite element results using Eq. (7). We note that excessively high stresses are apparent in both cases in regions where there is actually no material due to the singularity in the stress function. Figures 2c and 2f show the relaxed von Mises stress that results after application of the interpolation in Eq. (20). It is readily apparent that this prescription has removed the stress singularity in void regions while preserving the true stress state in solid material in addition to the continuous variation throughout intermediate values.

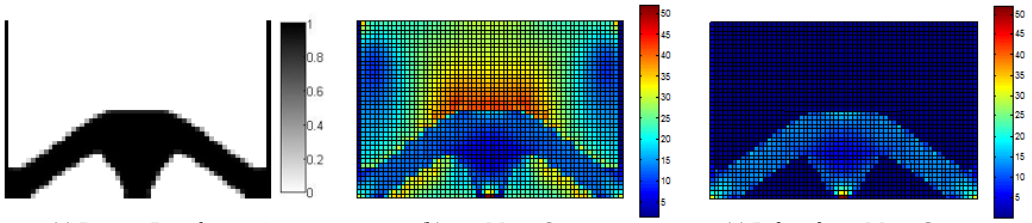

(a) Density Distribution 1 (b) von Mises Stress 1 (c) Relaxed von Mises Stress 1

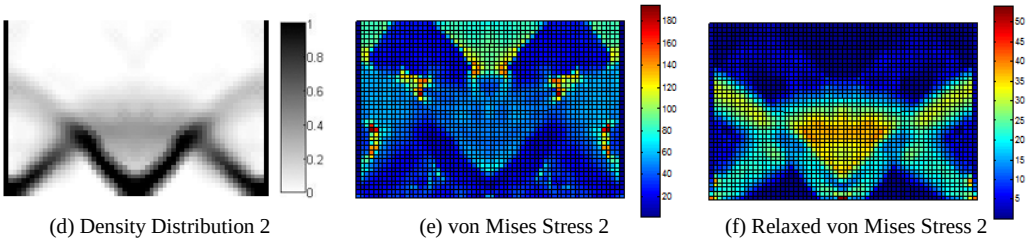

(d) Density Distribution 2 (e) von Mises Stress 2 (f) Relaxed von Mises Stress 2

Figure 2: Two arbitrary density distributions for a structure subjected to combined mechanical and temperature loads (a,d) along with the corresponding von Mises stress distributions (b,e) and relaxed von Mises stress distributions (c,f) using the interpolation in Eq. (20).

5.4. Stress Constraint Aggregation

Efficient computation of response sensitivities is paramount to any structural optimization process that employs a gradient-based optimization algorithm. Thus, a major challenge in stress-constrained problems is the large scope of the resulting optimization problem. Ideally, we wish to ensure the maximum stress within the design domain remains below constraint limits; however, the max operator is not differentiable because the location of maximum stress may jump from one element to another. In typical structural optimization, to ensure the maximum stress is controlled in the structure, a stress constraint can be placed on every element. However, in topology optimization, this creates a large number of constraints. Practical topology optimization problems generally include tens or even hundreds of thousands of variables, which results in an optimization problem with an equally large number of stress constraints. In this case, neither the direct nor the adjoint method for analytical sensitivity analysis is computationally efficient. A number of research works have successfully reduced the number of stress constraints by using aggregation functions to group the stresses throughout the model, or in regions of the structure, into aggregated stress measures. In this work, we utilize the *p-norm* function given by

$$\sigma_{PN} = \left[\sum_{e=1}^{N} \left(\frac{F(\boldsymbol{\sigma}_e)}{\sigma_{\text{lim}}} \right)^p \right]^{1/p} . \tag{20}$$

Here, p is an aggregation parameter that controls the level of smoothness of the aggregation, with $p \to \infty$ matching identically the maximum value within the aggregation set. However; to ensure an optimizer can efficiently navigate the design domain, the value of the aggregation parameter cannot become excessively large, which means that some accuracy in the local resolution of stress values. To remedy this for large problems, recently regionalized or block aggregated techniques have been proposed. In these methods, a number of regions are defined and aggregation functions are applied to the elements only within each region in an effort to regain some of the local accuracy at an acceptable level of computational cost. In this work, we utilize only a single aggregation function to demonstrate the basics of thermoelastic topology optimization with stresses. In the future, we plan to integrated regionalized measures for larger scale problems. To achieve better performance in this work, a continuation scheme is employed to slowly increase the p aggregation parameter during optimization.

6. Demonstration

6.1. Example Problem

The test problem we utilize here is inspired by the bi-clamped domain with combined mechanical and thermal loading first introduced by Rodrigues and Fernandes [3] and explored by various authors for compliance minimization in the presence of thermal loading. Figure 3 shows the design domain for the structure. It is discretized with four node bi-linear quadrilateral plane stress elements with 60 elements in the horizontal direction and 40 elements in the vertical direction. The elastic modulus of the material is $E = 210$ GPa, the coefficient of thermal expansion is $\alpha = 1.1\times10^{-5}/°C$, the Poisson's ratio is $\nu = 0.3$, and the thickness is taken as $t = 0.01$ m. Gray elements in the figure denote non-design regions in the model while white elements indicate the designable domain. A design-independent mechanical load of $F = 10$ kN is applied to the center of the bottom edge along with a uniform temperature increase of ΔT throughout. A small non-design region near the application of the mechanical point load is included to prevent a geometrical stress singularity.

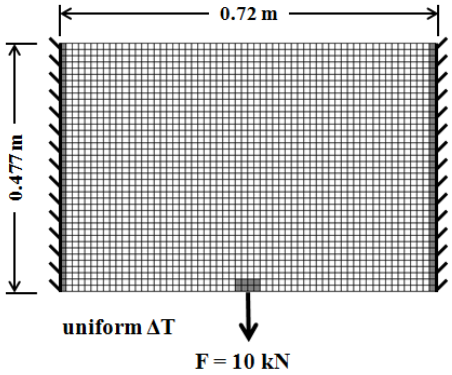

Figure 3: Bi-clamped structural domain with non-design (gray) and designable (white) regions.

The nonlinear optimization problem is solved using the MMA optimizer with an external move limit to prevent excessive step sizes and ensure smooth convergence. The aggregation parameter in the global stress constraint is increased from 10 to 50 using a continuation method and the interpolation parameters on stiffness and TSC are $q_E = 8$ and $q_\beta = 0$, respectively, in the results that follow.

6.2. Results

Figure 4 shows the results of both the stress-constrained topology problem along with the minimum compliance volume-constrained problem. In the stress-constrained problem, the limit stress for this set of results was taken to be $\sigma_{\text{lim}} = 20$ MPa and three different levels of temperature loading, $\Delta T = 1°C$ (left-column), $\Delta T = 0°C$, and $\Delta T = -1°C$ (right-column), are given. In order to determine how much volume to allow, the stress-constrained problem for each load was solved first and the resulting minimum volume was utilized as the volume constraint for the minimum compliance optimization for each load case.

In the figure, the density distributions for the stress-constrained problems corresponding to the three levels of temperature loading are given in the top row with the stress distribution for each directly below. The third row shows minimum compliance results for the same loading cases also with distributions of stress given below. Upon first inspection we note that in each case, the two problem formulations have produced different topological designs. We see that the stress-constrained problems have each satisfied the stress constraints and the minimum compliance design has resulted in structures with higher maximum stress values. The exception to this is for the structure with no thermal load applied. In the case of purely mechanically loaded structures, it is understood that a minimum compliance (maximum stiffness) design generally leads to suitable stress results with the exception of geometric singularities such as re-entrant corners. However, it is evident that the stress-constrained problem formulation produces structures with a much more uniform stress field. This indicates that in addition to naturally preventing geometric or loading singularities, the optimizer is able to identify optimal load paths for both external and internal loads (such as temperature loads). We note that the uniformly stressed structures generated by the stress-constrained optimization appear to be superior with respect to stresses when compared to the minimum compliance results. This conclusion is supported by other literature results including the work by Pedersen and Pedersen, who showed that thermoelastic structures optimized for uniform energy density showed more desirable strength characteristics than those optimized for maximum stiffness [14].

Another interesting observation related to the influence of elevated temperature is the relative compliance of

each structure. We see that for purely mechanical loading, the minimum compliance formulation produces a much stiffer design than does the stress-constrained problem. However, when thermal effects are included, there seems to be no advantage in terms of overall structural stiffness obtained by using the compliance minimization problem over the stress-constrained formulation. In fact, it appears that superior stress behavior can be obtained without sacrificing overall structural rigidity by simply allowing the optimizer to identify optimal connectivity for uniform stress.

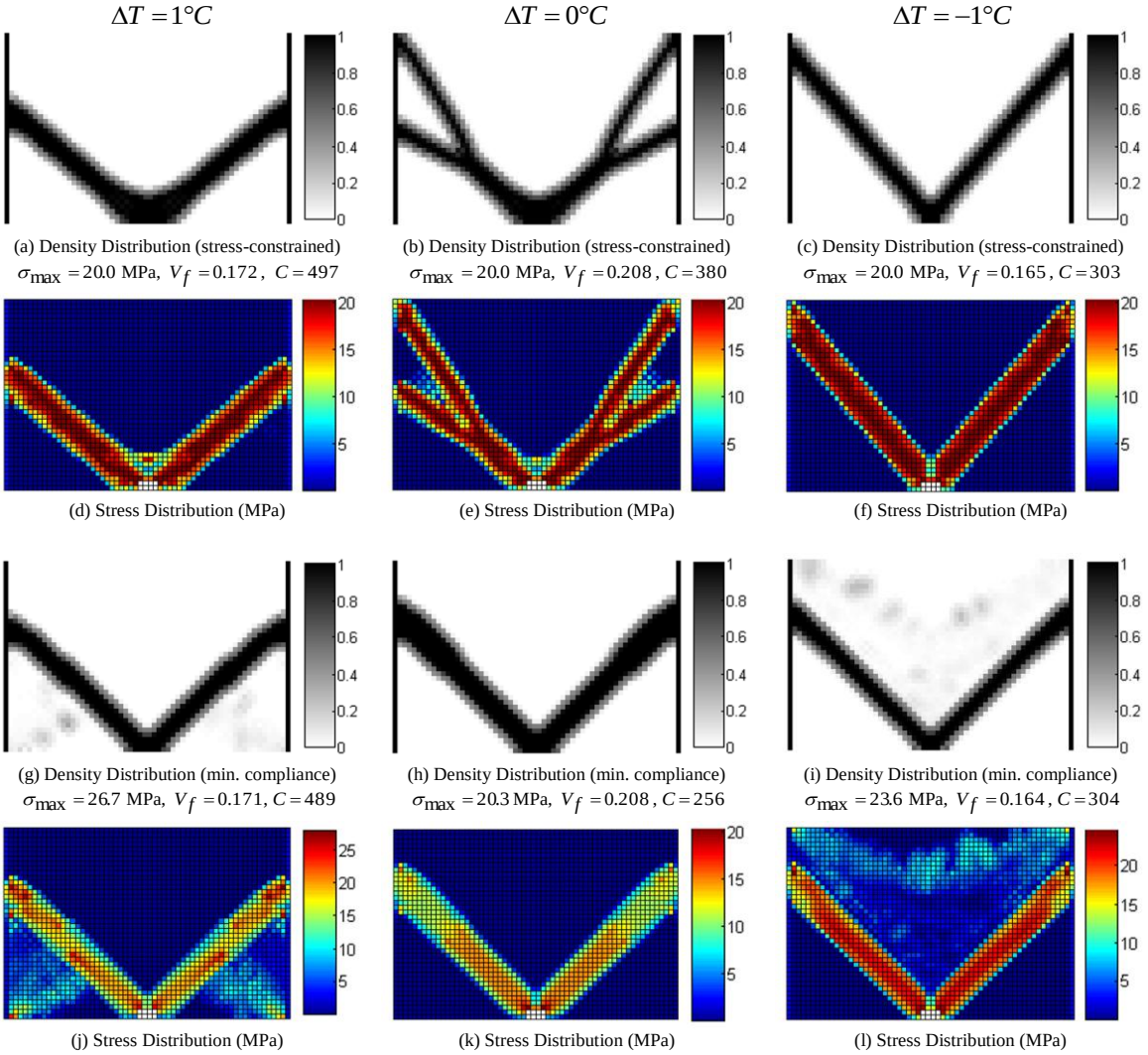

Figure 4: Comparison of density and stress distribution results obtained using stress-constrained optimization and minimum compliance optimization for three levels of temperature loading. Maximum stress, compliance, and volume fraction are given in the caption each design. Stress-constrained results are given in the top two rows of the figure while minimum compliance results for identical loading conditions are given in the bottom two rows.

Finally, the iteration history for the stress-constrained problem and the minimum compliance problem are given for the case of $\Delta T = 1°C$ in Figures 5a and 5b, respectively. We note that in both cases, the constraints are satisfied and the objective functions show convergence towards minima. This indicates that even for the highly nonlinear stress function the optimization algorithm can navigate the design space. We do note that the minimum compliance objective oscillates at convergence, which is a slight numerical issue with intermediate density material described previously. It appears that the design dependent loading creates an oscillating small positive/negative sensitivity in the objective near the minimum. In the future, more advanced projection methods, such as the Heaviside projection method of Guest may be investigated to reduce this numerical anomaly.

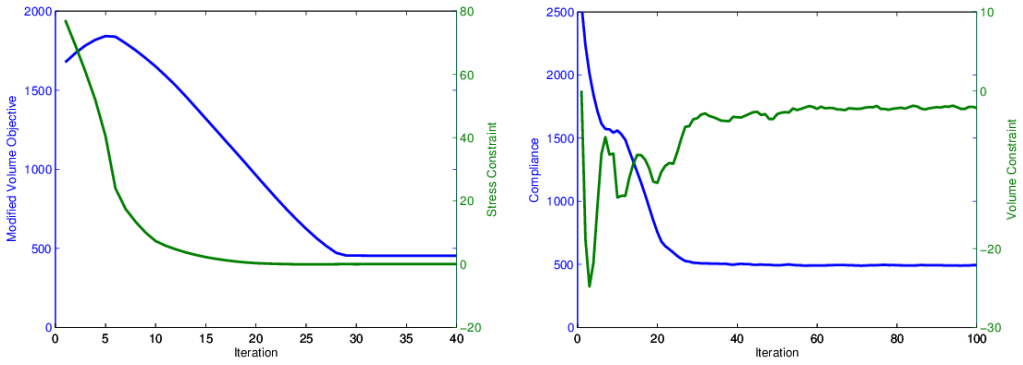

(a) Stress-constrained (b) Minimum Compliance

Figure 5: Iteration history for $\Delta T = 1°C$ for (a) stress-constrained optimization and (b) minimum compliance optimization.

7. Summary and Conclusions

In this paper we have demonstrated the application of stress constraints to structural topology optimization problems with thermal loading. This work is motivated by the lack of suitable design methods for structures that must operate in an elevated temperature design environment with strict fixivity requirements that prohibit thermal expansion and generate thermal stresses. Interpolation of the design-dependent thermal load in the topology optimization problem has been accomplished using the thermal stress coefficient and the singularity phenomenon in stress constraints has been circumvented using a modern technique based on a stress interpolation function. Results of both volume-constrained compliance minimization and stress-constrained volume minimization topology optimization problems have been obtained. Preliminary results indicate that the resulting topologies are different if thermal effects are a significant source of loading in the structure. It was also observed that less material was utilized by the stress-constrained topology optimization problems. This supports the conclusion that when designing against thermal stresses, using less structural material may produce lower thermal stresses because less material exists in the domain to generate thermal loading. Despite the computational advantage of traditional minimum compliance topology optimization, the stress-constrained volume minimizing problem formulation shows better performance and stability and does not appear to be as sensitive to numerical issues that arise from design-dependent loading. This includes the inability of the minimum compliance objective to achieve crisp black/white designs due to a non-active volume constraint. As a result, we conclude that stress-based design criteria in the topology optimization of thermal structures hold significant potential and provide an attractive avenue for future research and development.

In the future, this work will be extended to include the effects of geometric nonlinearity in the form of large displacements and follower forces, which can be characteristic of thermal structures problems with restrained thermal expansion. In addition, the actual temperature distributions on practical structures generally cannot be idealized as simply uniform temperature distributions. Thus, we wish to include the physics of heat transfer in the topology optimization process. It is important to note that this will required a coupled analysis procedure to capture the design dependency of the heat transfer, which can include combinations of conduction, convection, and radiation, on the structural configuration.

8. References

[1] M.P. Bendsoe and O. Sigmund, *Topology Optimization: Theory, Methods and Applications*, Springer-Verlag, Berlin, 2003.

[2] J.D. Deaton and R.V. Grandhi, A Survey of Structural and Multidisciplinary Continuum Topology Optimization: post 2000, *Structural and Multidisciplinary Optimization*, in 2nd review, 2013.

[3] H. Rodrigues and H. Fernandes, A material based model for topology optimization of thermoelastic structures, *International Journal for Numerical Methods in Engineering*, 38, 1951-1965, 1995.

[4] Q. Li, G.P. Steven, and Y.M. Xie, Displacement minimization of thermoelastic structures by evolutionary thickness designs," *Computer Method in Applied Mechanics and Engineering*, 179, 361-378, 1999.

[5] Q. Li, G.P. Steven, and Y.M. Xie, Thermoelastic topology optimization for problems with varying temperature fields, *Journal of Thermal Stresses*, 24, 347-366, 2001.

[6] W.Y. Kim, R.V. Grandhi, and M. Haney, Multi objective evolutionary structural optimization using combined static/dynamic control parameters. *AIAA Journal*, 44 (4), 794-802, 2006.

[7] R.C. Penmetsa, R.V. Grandhi, and M. Haney, Topology optimization for an evolutionary design of a thermal

protection system, *AIAA Journal*, 44 (11), 2664-2671, 2006.
[8] O. Sigmund and S. Torquato, Design of materials with extreme thermal expansion using a three-phase topology optimization method, *Journal of the Mechanics and Physics of Solids*, 45, 1037-1067, 1997.
[9] O. Sigmund, Design of multiphysics actuators using topology optimization - Part I: One-material structures, *Computer Methods in Applied Mechanics and Engineering*, 190, 6577-6604, 2001.
[10] C. Jog, Distributed-parameter optimization and topology design for non-linear thermoelasticity, *Computer Methods in Applied Mechanics and Engineering*, 132 (1-2), 117-134, 1996.
[11] T. Gao and W. Zhang, Topology optimization involving thermo-elastic stress loads, *Structural and Multidisciplinary Optimization*, 42, 725-738, 2010.
[12] Q. Xia and M.Y. Wang, Topology optimization of thermoelastic structures using the level set method, *Computational Mechanics*, 42 (6), 837-857, 2008.
[13] J. Yan, G.D. Cheng, and L. Liu, A uniform optimum material based model for concurrent optimization of thermoelastic structures and materials. *International Journal for Simulation and Multidisciplinary Design Optimization*, 2, 259-266, 2008.
[14] P. Pedersen and N.L. Pedersen, Strength optimized designs of thermoelastic structures, *Structural and Multidisciplinary Optimization*, 42, 681-691, 2010.
[15] P. Pedersen and N.L. Pedersen, Interpolation/penalization applied for strength design of 3D thermoelastic structures, *Structural and Multidisciplinary Optimization*, 45, 773-786, 2012.
[16] J.D. Deaton and R.V. Grandhi, Stiffening of restrained thermal structures via topology optimization, *Structural and Multidisciplinary Optimization*, DOI: 10.1007/s00158-013-0934-5, 2013.
[17] B. Wang, J. Yan, and G. Cheng, Optimal structure design with low thermal directional expansion and high stiffness, *Engineering Optimization*, 43 (6), 581-595, 2011.
[18] M.A. Haney and R.V. Grandhi, Consequences of Material Addition for a Beam Strip in a Thermal Environment, *AIAA Journal*, 47 (4), 1026-1034, 2009.
[19] C. Le, J. Norato, T. Bruns, C. Ha, and D. Tortorelli, Stress-based topology optimization for continua, *Structural and Multidisciplinary Optimization*, 41, 605-620, 2010.
[20] P. Duysinx and M.P. Bendsoe, Topology optimization of continuum structures with local stress constraints, *International Journal for Numerical Methods in Engineering*, 43 (2), 1453-1478, 1998.
[21] P. Duysinx and M.P. Bendsoe, New development in handling stress constraints in optimal material distribution, *7th AIAA/USAF/NASA/ISSMO Symposium on Multidisciplinary Analysis and Optimization*, St. Louis, Missouri, 3, 1501-1509, 1998.
[22] J.T. Pereira, J.T., E.A. Fancello, and C.S. Barcellos, Topology optimization of continuum structures with material failure constraints, *Structural and Multidisciplinary Optimization*, 26, 50-66, 2004.
[23] M. Bruggi, On an alternative approach to stress constraints relaxation in topology optimization, *Structural and Multidisciplinary Optimization*, 36, 125-141, 2008.
[24] M. Bruggi and P. Duysinx, A stress-based approach to the optimal design of structures with unilateral behavior of material or supports, *Structural and Multidisciplinary Optimization*, DOI 10.1007/s00158-013-0896-7, 2013.
[25] C.E.M. Guilherme and J.S.O. Fonseca, Topology optimization of continuum structures with ε-relaxed stress constraints, *Solid Mechanics in Brazil*, 1, 239-250, 2007.
[26] París, J. and F. Navarrina, I. Colominas, and M. Casteleiro, Block aggregation of stress constraints in topology optimization of structures, *Advances in Engineering Software*, 41, 433-441, 2010.
[27] París, J. and F. Navarrina, I. Colominas, and M. Casteleiro, Improvements in the treatment of stress constraints in structural topology optimization problems, *Journal of Computational and Applied Mathematics*, 234, 2231-2238, 2010.
[28] E. Lee, K.A. James, and J.R.R.A. Martins, Stress-constrained topology optimization with design-dependent loading, *Structural and Multidisciplinary Optimization*, 46, 647-661, 2012.
[29] K. Suresh and M. Takalloozadeh, Stress-constrained topology optimization: a topological level-set approach, *Structural and Multidisciplinary Optimization*, DOI 10.1007/s00158-013-0899-4, 2013.
[30] E. Holmberg, B. Torstenfelt, and A. Klarbring, Stress constrained topology optimization, *Structural and Multidisciplinary Optimization*, DOI 10.1007/s00158-012-0880-7, 2013.
[31] M. Stolpe and K. Svanberg, An alternative interpolation scheme for minimum compliance topology optimization, *Structural and Multidisciplinary Optimization*, 22, 116-124, 2001.
[32] M. Bruyneel and P. Duysinx, Note on topology optimization of structures including self-weight, *Structural and Multidisciplinary Optimization*, 29 (4), 245-256, 2005.
[33] T.E. Bruns and D.A. Tortorelli, Topology optimization of non-linear elastic structures and compliant mechanisms, *Computer Methods in Applied Mechanics and Engineering*, 190 (26-27), 3443-3459, 2001.
[34] K. Svanberg, The method of moving asymptotes - a new method for structural optimization, *International Journal for Numerical Methods in Engineering*, 24, 359-373, 1987.